

Response of dust emissions in southwestern North America to 21st century trends in climate, CO₂ fertilization, and land use: implications for air quality

Yang Li, Loretta J. Mickley, Jed O. Kaplan

Angaben zur Veröffentlichung / Publication details:

Li, Yang, Loretta J. Mickley, and Jed O. Kaplan. 2021. "Response of dust emissions in southwestern North America to 21st century trends in climate, CO₂ fertilization, and land use: implications for air quality." *Atmospheric Chemistry and Physics* 21 (1): 57-68. <https://doi.org/10.5194/acp-21-57-2021>.



Response of dust emissions in southwestern North America to 21st century trends in climate, CO₂ fertilization, and land use: implications for air quality

Yang Li¹, Loretta J. Mickley¹, and Jed O. Kaplan²

¹John A. Paulson School of Engineering and Applied Sciences, Harvard University, Cambridge, MA, USA

²Department of Earth Sciences, The University of Hong Kong, Hong Kong SAR, China

Correspondence: Yang Li (yangli@seas.harvard.edu)

Received: 1 April 2020 – Discussion started: 15 April 2020

Revised: 1 October 2020 – Accepted: 5 November 2020 – Published: 4 January 2021

Abstract. Climate models predict a shift toward warmer and drier environments in southwestern North America. The consequences of such a shift for dust mobilization and dust concentration are unknown, but they could have large implications for human health, given the connections between dust inhalation and disease. Here we link a dynamic vegetation model (LPJ-LMfire) to a chemical transport model (GEOS-Chem) to assess the impacts of future changes in three factors – climate, CO₂ fertilization, and land use practices – on vegetation in this region. From there, we investigate the impacts of changing vegetation on dust mobilization and assess the net effect on fine dust concentration (defined as dust particles less than 2.5 μm in diameter) on surface air quality. We find that surface temperatures in southwestern North America warm by 3.3 K and precipitation decreases by nearly 40 % by 2100 in the most extreme warming scenario (RCP8.5; RCP refers to Representative Concentration Pathway) in spring (March, April, and May) – the season of greatest dust emissions. Such conditions reveal an increased vulnerability to drought and vegetation die-off. Enhanced CO₂ fertilization, however, offsets the modeled effects of warming temperatures and rainfall deficit on vegetation in some areas of the southwestern US. Considering all three factors in the RCP8.5 scenario, dust concentrations decrease over Arizona and New Mexico in spring by the late 21st century due to greater CO₂ fertilization and a more densely vegetated environment, which inhibits dust mobilization. Along Mexico's northern border, dust concentrations increase as a result of the intensification of anthropogenic land use. In contrast, when CO₂ fertilization is not considered in the RCP8.5 scenario, vege-

tation cover declines significantly across most of the domain by 2100, leading to widespread increases in fine dust concentrations, especially in southeastern New Mexico (up to ~2.0 μg m⁻³ relative to the present day) and along the border between New Mexico and Mexico (up to ~2.5 μg m⁻³). Our results have implications for human health, especially for the health of the indigenous people who make up a large percentage of the population in this region.

1 Introduction

The arid and semiarid region covering the southwestern US and northwestern Mexico is characterized by large concentrations of soil-derived dust particles in the lower atmosphere, especially in spring (Hand et al., 2016). By causing respiratory and cardiovascular diseases, fine dust particles – i.e., those particles with diameter less than 2.5 μm (PM_{2.5}) – can have negative effects on human health (Tong et al., 2017; Meng and Lu, 2007; Gorris et al., 2018). A key question is to what extent will climate change and other factors influence future dust concentrations in this region, which we define here as southwestern North America. In this study, we use a suite of models to predict the future influence of three factors – climate change, increasing CO₂ fertilization, and land use change – on vegetation in this region, and we assess the consequences for dust mobilization and dust concentrations.

Wind speed and vegetation cover are two key factors that determine soil erodibility and dust emissions. Wind gusts mobilize dust particles from the Earth's surface, whereas

vegetation constrains dust emissions by reducing the extent of bare land and preserving soil moisture (Zender et al., 2003). The high temperatures and reduced soil moisture characteristic of drought play an important role in dust mobilization, as the loss of vegetative cover during drought increases soil erosion (Archer and Predick, 2008; Bestelmeyer et al., 2018).

Southwestern North America is covered by desert grassland, perennial grassland, savanna, desert scrub, and grassy shrublands or woodlands (McClaran and Van Devender, 1997). In recent decades, a gradual transition from grasslands to shrubland has been observed across much of this region, with increased aridity, atmospheric CO₂ enrichment, and livestock grazing all possibly playing a role in this trend (Bestelmeyer et al., 2018). Future climate change may further prolong this transition, especially as shrubs fare better than grasses under a climate regime characterized by large fluctuations in annual precipitation (Bestelmeyer et al., 2018; Edwards et al., 2019). Climate models predict a warmer and drier environment in southwestern North America through the 21st century, with more frequent and severe drought (Seager and Vecchi, 2010; MacDonald, 2010; Stahle, 2020; Prein et al., 2016; Williams et al., 2020). Such conditions would decrease vegetative cover and allow for greater dust mobilization. On the other hand, elevated CO₂ concentrations in the future atmosphere could increase photosynthesis and decrease transpiration of some vegetation species, allowing for more efficient water use and enhancing growth (Poorter and Perez-Soba, 2002; Polley et al., 2013). Anthropogenic land use practices – e.g., agriculture, human settlement, and urban sprawl – have changed dramatically over southwestern North America in recent decades, with Arizona and New Mexico showing decreasing cropland area and northern Mexico experiencing increasing pasture area (Fig. S1 in the Supplement). Future land use practices could also influence the propensity for dust mobilization by disturbing crustal biomass (e.g., Belnap and Gillette, 1998).

Previous studies have investigated the relative importance of climate, CO₂ fertilization, and/or land use in present-day and future dust emissions and concentrations, sometimes with contradictory results. For example, Woodward et al. (2005) predicted a tripling of the global dust burden by 2100 relative to the present day, whereas other studies suggested a decrease in the global dust burden (e.g., Harrison et al., 2001; Mahowald and Luo, 2003; Mahowald et al., 2006). These estimates of future dust emissions depended in large part on the choice of model applied, as demonstrated by Tegen et al. (2004).

In southwestern North America, a few recent studies have examined statistical relationships between observed present-day dust concentrations and meteorological conditions or leaf area index (LAI). Hand et al. (2016) found that fine dust concentrations in spring in this region correlated with the Pacific Decadal Oscillation (PDO), indicating the importance of large-scale climate patterns in the mobilization and trans-

port of regional fine dust. Tong et al. (2017) further determined that the observed 240 % increase in the frequency of windblown dust storms from the 1990s to the 2000s in the southwestern US was likely associated with the PDO. Similarly, Achakulwisut et al. (2017) found that the 2002–2015 increase in average March fine dust concentrations in this region was driven by a combination of positive PDO conditions and phase of the El Niño–Southern Oscillation. More recently, Achakulwisut et al. (2018) identified the standardized precipitation–evapotranspiration index as a useful indicator of present-day dust variability. Applying that metric to an ensemble of future climate projections, these authors predicted increases of 26 %–46 % in fine dust concentrations over the southwestern US in spring by 2100. In contrast, Pu and Ginoux (2017) found that the frequency of extreme dust days decreases slightly in spring in this region due to the reduced extent of bare land under 21st century climate change.

These regional studies relied mainly on statistical models that relate local and/or large-scale meteorological conditions to dust emissions in southwestern North America. Pu and Ginoux (2017) also considered changing LAI in their model, but these dust–LAI relationships were derived from a relatively sparse dataset, casting some uncertainty on the results (Achakulwisut et al., 2018). In this study, we investigate the effects of climate change, increasing CO₂ fertilization, and future land use practices on vegetation in southwestern North America, and we examine the response of dust mobilization due to these changes in vegetation. With regard to climate, we examine whether a shift to warmer, drier conditions by 2100 enhances dust mobilization in this region by reducing vegetation cover and exposing bare land. To that end, we couple the LPJ-LMfire dynamic vegetation model to the GEOS-Chem chemical transport model to study vegetation dynamics and dust mobilization under different conditions and climate scenarios, allowing for the consideration of several factors driving future dust mobilization in southwestern North America. We focus on fine dust particles in springtime (March, April, and May), because it is the season with the highest dust concentrations in the southwestern US (Hand et al., 2017). Given the deleterious impacts of airborne dust on human health, our dust projections under different climate scenarios have value for understanding the full array of potential consequences of anthropogenic climate change.

2 Methods

We examine dust mobilization in southwestern North America, here defined as the area from 25 to 37° N and from 100 to 115° W (Fig. 1), during the late 21st century under scenarios of future climate and land use based on two Representative Concentration Pathways (RCPs). RCP4.5 and RCP8.5 capture two possible climate trajectories over the 21st century, beginning in 2006. RCP4.5 represents a scenario of moderate future climate change with a gradual reduction in green-

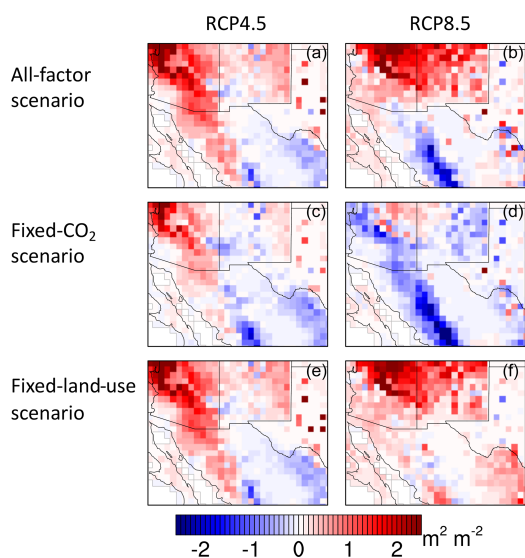


Figure 1. Simulated changes in spring averaged monthly mean vegetation area index (VAI) in southwestern North America under the three conditions for RCP4.5 and RCP8.5. Changes are between the present day and 2100, with 5 years representing each time period. The all-factor case (a, b) includes the effects of climate, CO₂ fertilization, and anthropogenic land use on vegetation; only climate and land use are considered in the fixed-CO₂ case (c, d); and only climate and CO₂ fertilization are considered in the fixed-land-use case (e, f). Results are from LPJ-LMfire.

house gas (GHG) emissions after 2050 and a radiative forcing at 2100 relative to preindustrial values of $+4.5 \text{ W m}^{-2}$, whereas RCP8.5 represents a more extreme scenario with continued increases in GHGs throughout the 21st century and a radiative forcing of $+8.5 \text{ W m}^{-2}$ at 2100. For each RCP, we investigate the changes in vegetation for three cases: (1) an all-factor case that includes changes in climate, land use, and CO₂ fertilization; (2) a fixed-CO₂ case that includes changes in only climate and land use; and (3) a fixed-land-use case that includes changes in only climate and CO₂ fertilization.

We use LPJ-LMfire, a dynamic global vegetation model, to estimate changes in vegetation under future conditions (Pfeiffer et al., 2013). Meteorology to drive LPJ-LMfire is taken from the Goddard Institute for Space Studies (GISS) climate model (Nazarenko et al., 2015). Using the GEOS-Chem Harvard–NASA Emissions Component (HEMCO), we then calculate dust emissions based on the LPJ-generated vegetation area index (VAI) for all scenarios. We apply the resulting dust emissions to the GEOS-Chem global chemical transport model to simulate the distribution of fine dust across southwestern North America.

2.1 GISS ModelE

Present-day and future meteorological fields for RCP4.5 and RCP8.5 are simulated by the GISS ModelE climate model (Nazarenko et al., 2015), configured for Phase 5 of the

Coupled Model Intercomparison Project (CMIP5; <https://esgf-node.llnl.gov/search/cmip5/>, last access: 17 July 2020). The simulations cover the years from 1801 to 2100 at a spatial resolution of 2° latitude \times 2.5° longitude. Changes in climate in the GISS model are driven by increasing greenhouse gases. In RCP4.5, CO₂ concentrations increase to 550 ppm by 2100; in RCP8.5 the CO₂ increases to 1960 ppm (Meinshausen et al., 2011).

Under RCP4.5, the GISS model predicts a slight increase of 0.45 K in the springtime mean surface temperatures and an increase in mean precipitation of $\sim 17\%$ over southwestern North America by the 2100 time slice (2095–2099), relative to the present day (2011–2015). In contrast, under RCP8.5, the 5-year mean springtime temperature increases significantly (by 3.29 K) by 2100 and mean precipitation decreases by $\sim 39\%$. The spatial distributions of the changes in temperature and precipitation by 2100 under RCP8.5 are presented in the Supplement (Fig. S2). In addition, lightning strike densities decrease by ~ 0.006 strikes $\text{km}^{-2} \text{d}^{-1}$ over Arizona in RCP4.5, but they increase by the same magnitude in this region in RCP8.5 (Li et al., 2020). Lightning strikes play a major role in wildfire ignition in this region, and wildfires may influence landscape succession (e.g., Bodner and Robles, 2017). Finally, future surface wind speeds do not change significantly under RCP4.5, but they increase slightly by $\sim 4\%$ across southwestern North America under RCP8.5 by 2100 (not shown). The increasing winds in RCP8.5 will influence the spread of fires in our study, but they will not affect the simulated dust fluxes directly, as described in more detail below. Compared with predictions from other climate models, the GISS projections of climate change in southwestern North America are conservative (Ahlström et al., 2012; Sheffield et al., 2013), implying that our predictions of the impact of climate change on dust mobilization may also be conservative.

In our study, we do not specifically track drought frequency under future climate, as the definition of drought is elusive (Andreadis et al., 2005; Van Loon et al., 2016). Nonetheless, the meteorological conditions predicted in the RCP8.5 scenario for 2100 align with previous studies projecting an increased risk of drought in this region (e.g., Williams et al., 2020), and, as we shall see, such conditions, in the absence of CO₂ fertilization, result in decreased vegetation and greater dust mobilization.

2.2 LPJ-LMfire

LPJ-LMfire is a dynamic vegetation model that includes a process-based representation of fire (Pfeiffer et al., 2013). Input to LPJ-LMfire includes meteorological variables, soil characteristics, land use, and atmospheric CO₂ concentrations, and the model then simulates the corresponding vegetation structure, biogeochemical cycling, and wildfire at a spatial resolution of 0.5° latitude \times 0.5° longitude. Here

“vegetation structure” refers to vegetation types and the spatial patterns in landscapes.

More specifically, LPJ-LMfire simulates the impacts of photosynthesis, evapotranspiration, and soil water dynamics on vegetation structure and the population densities of different plants functional types (PFTs). The model considers the coupling of different ecosystem processes, such as the interactions between CO₂ fertilization, evapotranspiration, and temperature as well as the competition among different PFTs for water resources (e.g., precipitation, surface runoff, and drainage). The different PFTs in LPJ-LMfire respond differentially to changing CO₂, with CO₂ enrichment preferentially stimulating photosynthesis in woody vegetation and C₃ grasses compared with C₄ grasses (Polley et al., 2013). Wildfire in LPJ-LMfire depends on lightning ignition, and the simulation considers multiday burning, coalescence of fires, and the spread rates of different vegetation types. The effects of changing fire activity on vegetation cover are then taken into account (Pfeiffer et al., 2013; Sitch et al., 2003; Chaste et al., 2019). Li et al. (2020) predicted a ~ 50 % increase in fire-season area burned by 2100 under scenarios of both moderate and intense future climate change over the western US. However, the effects of changing fire on vegetation cover are insignificant in the grass- and bare-ground-dominated ecosystems of the desert Southwest, where low biomass fuels cannot support the extensive spread of fires.

For this study we follow Li et al. (2020) and link meteorology from GISS-E2-R to LPJ-LMfire in order to capture the effects of climate change on vegetation. Meteorological fields from the GISS model include monthly mean surface temperature, diurnal temperature range, total monthly precipitation, number of days in the month with precipitation greater than 0.1 mm, monthly mean total cloud cover fraction, and monthly mean surface wind speed. Monthly mean lightning strike density, calculated using the GISS convective mass flux and the empirical parameterization of Magi (2015), is also applied to LPJ-LMfire. To downscale the 2° × 2.5° GISS meteorology to a finer resolution for LPJ-LMfire, we calculate the 2010–2100 monthly anomalies relative to the average over the 1961–1990 period, and we then add these anomalies to an observationally based climatology (Pfeiffer et al., 2013). LPJ-LMfire then simulates the response of natural vegetation to the 21st century trends in these meteorological fields and to increasing CO₂. We apply the same changes in CO₂ concentrations as those applied to the GISS model.

We overlay the changes in natural land cover with future land use scenarios from CMIP5 (Hurt et al., 2011; <http://tntcat.iiasa.ac.at/RcpDb/>, last access: 17 July 2020). Such land use includes agriculture, human settlement, and urban sprawl – all of which result in habitat loss and the fragmentation of forested landscapes. Present-day land use prepared for CMIP5 is taken from the HYDE database v3.1 (Klein Goldewijk, 2001; Klein Goldewijk et al., 2011), which, in turn, is based on an array of sources, including satellite observations and government statistics. In our simulations, fire is not

allowed to occur on cropland or rangeland, so we do consider some land management. On the other hand, our model does not account for the density of livestock on rangeland, which, when mismanaged, can lead to a reduction in vegetation cover and enhanced dust emissions. In RCP8.5, the extent of cropland and pasture cover increases by ~ 30 % in Mexico but decreases by 10 %–20 % over areas along Mexico’s northern border in the US (Hurt et al., 2011). Only minor changes in land use practices by 2100 are predicted under RCP4.5 (Hurt et al., 2011).

We perform global simulations with LPJ-LMfire on a 0.5° × 0.5° grid for the two RCPs from 2006 to 2100, and we analyze results over southwestern North America, where dust emissions are especially high. For each RCP, we consider the effects of changing climate on land cover as well as the influence of anthropogenic land use change and CO₂ fertilization. The LPJ-LMfire simulations yield monthly time series of the leaf area indices (LAI) and fractional vegetation cover (σ_v) for nine plant functional types (PFTs): tropical broadleaf evergreen, tropical broadleaf raingreen, temperate needleleaf evergreen, temperate broadleaf evergreen, temperate broadleaf summergreen, boreal needleleaf evergreen, and boreal summergreen trees, as well as C₃ and C₄ grasses. We further discuss the LPJ-LMfire present-day land cover in the Supplement.

2.3 Vegetation area index calculation

Vegetation constrains dust emissions in two ways: (1) by competing with bare ground as a sink for atmospheric momentum, which results in less drag on erodible soil (Nicholson et al., 1998; Raupach, 1994), and (2) by enhancing soil moisture through plant shade and root systems (Hillel, 1982). Here, we implement the dust entrainment and deposition (DEAD) scheme of Zender et al. (2003) to compute a size-segregated dust flux, which includes entrainment thresholds for saltation, moisture inhibition, drag partitioning, and saltation feedback. The scheme assumes that vegetation suppresses dust mobilization by linearly reducing the fraction of bare soil exposed in each grid cell:

$$A_m = (1 - A_l - A_w)(1 - A_s)(1 - A_v), \quad (1)$$

where A_l is the fraction of land covered by lakes, A_w is the fraction covered by wetlands, A_s is the fraction covered by snow, and A_v is the fraction covered by vegetation.

For this study, we use the VAI as a metric to represent vegetation because it includes not only leaves but also stems and branches, all of which constrain dust emission. The VAI is used to calculate A_v in Eq. (1) as follows:

$$A_v = \min[1.0, \min(\text{VAI}, \text{VAI}_t) / \text{VAI}_t], \quad (2)$$

where VAI_t is the threshold for the complete suppression of dust emissions – set here to 0.3 m² m⁻² (Zender et al., 2003; Mahowald et al., 1999).

To compute the dust fluxes, we need to convert the LAI from LPJ-LMfire to the VAI. The VAI is generally defined as the sum of the LAI plus the stem area index (SAI). Assuming immediate removal of all dead leaves, the fractional vegetation cover, σ_v , can be used to represent the SAI for the different PFTs (Zeng et al., 2002). Given that the threshold VAI_t for no dust emission is relatively low ($0.3 \text{ m}^2 \text{ m}^{-2}$), leaf area dominates stem area in the suppression of dust mobilization in the model. In areas where the LAI is greater than the SAI, we assume that the SAI does not play a role in controlling dust emissions, and we set the LAI equivalent to the VAI. We also assume that C₃ and C₄ grasses have zero stem area to avoid overestimating the VAI during the winter and early spring when such grasses are dead. Based on the method of Zeng et al. (2002), with modifications, we calculate the VAI in each grid cell as follows:

$$\text{VAI} = \max \left(\sum_{\text{PFT}=1}^9 \text{LAI} \sum_{\text{PFT}=1}^7 \sigma_v \right), \quad (3)$$

where the LAI is for the nine PFTs from LPJ-LMfire, and σ_v is for just seven PFTs, with σ_v for C₃ and C₄ grasses not considered. Of the nine PFTs, temperate needleleaf evergreen, temperate broadleaf evergreen, temperate broadleaf summergreen, and C₃ grasses dominate the region, with temperate needleleaf evergreen having the highest LAI in spring. This mix of vegetation type is consistent with observations (e.g., McClaran and Van Devender, 1997).

2.4 Calculation of dust emissions

Dust emissions are calculated offline in the DEAD dust mobilization module within the Harvard–NASA Emissions Component (HEMCO). We feed both the VAI generated by LPJ-LMfire and meteorological fields from the Modern-Era Retrospective analysis for Research and Applications (MERRA-2) at a spatial resolution of 0.5° latitude \times 0.625° longitude into the DEAD module (Gelaro et al., 2017). Dust emission is nonlinear with surface wind speed. Following Ridley et al. (2013), we characterize subgrid-scale surface winds as a Weibull probability distribution, which allows saltation even when the grid-scale wind conditions are below some specified threshold speed. The scheme assumes that the vertical flux of dust is proportional to the horizontal saltation flux, which, in turn, depends on surface friction velocity and the aerodynamic roughness length Z_0 . As recommended by Zender et al. (2003), and consistent with Fairlie et al. (2007) and Ridley et al. (2013), we uniformly set Z_0 to $100 \mu\text{m}$ across all dust candidate grid cells.

With this model setup, we calculate hourly dust emissions for two 5-year time slices for each RCP and condition, covering the present day (2011–2015) and the late 21st century (2095–2099). Dust emissions are generated for four size bins with respective radii of 0.1–1.0, 1.0–1.8, 1.8–3.0, and 3.0–6.0 μm . These dust emissions are then applied to GEOS-

Chem. The calculated present-day VAI and fine dust emissions are shown in Fig. S3, and we compare the modeled VAI with that observed in Figs. S4 and S5.

2.5 GEOS-Chem

We use the aerosol-only version of the GEOS-Chem chemical transport model (version 12.0.1; <http://acmg.seas.harvard.edu/geos/>, last access: 16 December 2020). For computational efficiency, we apply monthly mean oxidants archived from a full-chemistry simulation (Park et al., 2004). To isolate the effect of changing dust mobilization on air quality over southwestern North America, we use present-day MERRA-2 reanalysis meteorology from the NASA Global Modeling and Assimilation Office (Gelaro et al., 2017) for both the present-day and future GEOS-Chem simulations. In other words, we neglect the direct effects of future changes in wind speeds on dust mobilization, allowing us to focus instead on the indirect effects of changing vegetation on dust. For each time slice, we first carry out a global GEOS-Chem simulation at a 4° latitude \times 5° longitude spatial resolution; we then downscale to $0.5^\circ \times 0.625^\circ$ via grid nesting over the North American domain. In this study, we focus only on dust particles in the finest size bin (i.e., with radii of 0.1–1.0 μm), as these are most deleterious to human health. We compare modeled fine dust concentrations over southwestern North America for the present day against observations from the Interagency Monitoring of Protected Visual Environments (IMPROVE) network in Figs. S6–S7.

3 Results

3.1 Spatial shifts in the springtime vegetation area index

Figure 1 shows large changes in the spatial distribution of the modeled springtime VAI in southwestern North America for the three cases under both RCPs by 2100. In RCP4.5, the distributions of changes in the VAI are similar for the all-factor and fixed-land-use cases. Strong enhancements (up to $\sim 2.5 \text{ m}^2 \text{ m}^{-2}$) extend across much of Arizona, especially in the northwestern corner. The model exhibits moderate VAI increases in most of New Mexico and in the forest regions along the coast of northwestern Mexico. We find decreases in the modeled VAI (up to $\sim -1.6 \text{ m}^2 \text{ m}^{-2}$) in the southwestern corner of New Mexico, to the east of the coastal forests in Mexico, and in the forest regions near the Mexican border connecting with southern Texas. The similarity between the all-factor and fixed-land-use cases indicates the relatively trivial influence of land use change on vegetation cover in RCP4.5, compared with the effects of climate change and CO₂ fertilization. For the fixed-CO₂ case, western New Mexico and northern Mexico show greater decreases in the VAI, indicating how CO₂ fertilization in the other two cases offsets the effects of the warmer, drier climate on vegetation in

this region. Figure S8 further illustrates the strong positive impacts that CO₂ fertilization has on the VAI.

Compared with RCP4.5, the RCP8.5 scenario shows larger changes in climate, CO₂ concentrations, and land use by 2100 (Fig. 1). The net effects of these changes on vegetation are complex. As in RCP4.5, Arizona experiences a strong increase in the VAI in the all-factor and fixed-land-use cases, but this increase now extends to New Mexico. In contrast to RCP4.5, the modeled VAI decreases in the coastal forest areas in northern Mexico in the all-factor case for RCP8.5. In the fixed-land-use case, however, the VAI decrease in northern Mexico is nearly erased, indicating the role of vegetation and forest degradation caused by land use practices in this area (Fig. S9). For the fixed-CO₂ case for RCP8.5, the VAI decreases in nearly all of southwestern North America, except the northeastern corner of Arizona and the northwestern corner of New Mexico.

To better understand the changes in the VAI, we can examine changes in the LAI, which represents the major portion of the VAI, for the four dominant plant functional types (PFTs) in this region. For example, decreases in the LAI in the fixed-CO₂ case under RCP8.5 are dominated by the loss of temperate broadleaf evergreen (TeBE) and temperate broadleaf summergreen (TeBS) (Fig. S10). Temperate needleleaf evergreen (TeNE) shows areas of increase in the northern part and south of Texas in this scenario, while both TeBE and TeBS show increases in northern Arizona and New Mexico. In other areas, TeBS reveals strong decreases, especially in southern Arizona and Mexico. As predicted by previous studies (Bestelmeyer et al., 2018; Edwards et al., 2019), C₃ perennial grasses (C_{3gr}) in this case decrease across a large swath extending from Arizona through Mexico, showing the impacts of warmer temperatures and reduced precipitation, as well as (for Mexico) land use change. Increased fire activity also likely plays a role in the simulated decreases of forest cover and C₃ grasses for RCP8.5 in southern Arizona, where fires and drought may have affected landscape succession (Williams et al., 2013; Bodner and Robles, 2017). We also investigate trends in the LAI for different months in spring from the present day to 2100. We find that the greatest percentage decreases in TeBS and C₃ grasses occur in May, consistent with the largest decreases in precipitation in that month (not shown).

In summary, we find that the warmer and drier conditions of the future climate strongly reduce vegetation cover by 2100, especially in RCP8.5. In addition, CO₂ fertilization and land use practices further modify future vegetation, although in opposite ways, as illustrated by Fig. S8. Under a warmer climate, higher CO₂ concentrations facilitate vegetation growth everywhere in southwestern North America, with larger VAI increases occurring over Arizona and New Mexico. Combined changes in anthropogenic land use – including cropland, pasture, and urban area – are greater under RCP8.5 than under RCP4.5, with large increases in RCP8.5 across Mexico but only modest changes in Arizona, New

Mexico, and Texas (Fig. S9). The increases in Mexico result in the fragmentation of forested landscapes and decrease the VAI, especially in coastal forest regions and along the border with the US.

3.2 Spatial variations in spring fine dust emissions

Unlike the widespread changes in the VAI, future changes in fine dust emissions are concentrated in a few arid areas, including (1) the border regions connecting Arizona, New Mexico, and northern Mexico (hereafter referred to as the ANM border); (2) eastern New Mexico; and (3) western Texas (Fig. 2). In RCP4.5, slight increases in fine dust emission (up to $\sim 0.3 \text{ kg m}^{-2}$ per month) are simulated in the ANM border region in all the three cases. In contrast, fine dust emissions decrease by up to $\sim -1.0 \text{ kg m}^{-2}$ per month in eastern New Mexico and western Texas in RCP4.5 due to warmer temperatures and increasing VAI. Consistent with the modest changes in the VAI (Fig. 1), the three cases in RCP4.5 do not exhibit large differences, with only the fixed-CO₂ case showing slightly greater increases in dust emissions along the ANM border and in western Texas. In RCP8.5 in the all-factor case, spring fine dust emissions increase slightly by up to $\sim 0.4 \text{ kg m}^{-2}$ per month along the ANM border, but they decrease more strongly in western Texas by up to $\sim -1.4 \text{ kg m}^{-2}$ per month (Fig. 2). In contrast, the sign of the change in dust emissions reverses for the fixed-CO₂ case, with significant emission increases along the ANM border and in New Mexico. The area with decreasing emissions in western Texas also shrinks in the fixed-CO₂ case. These trends occur due to the climate stresses – e.g., warmer temperatures and decreased precipitation – that impair the growth of temperate broadleaf trees and C₃ grasses. In this case, such stresses are not offset by CO₂ fertilization (Fig. S10).

Figure 3 more vividly shows the opposing roles of CO₂ fertilization and projected land use change in southwestern North America. In RCP8.5, changing CO₂ fertilization alone promotes vegetation growth and dramatically reduces dust mobilization by up to $\sim -1.2 \text{ kg m}^{-2}$ per month. Figure 3 also reveals that land use trends are a major driver of increased dust emissions along the ANM border and in western Texas in RCP8.5, as croplands and rangelands expand in this region and temperate broadleaf trees decline (Hurt et al., 2011). Similarly, the expansion of rangelands in northern Mexico in RCP8.5 reduces natural vegetation cover there (Hurt et al., 2011), contributing to the increase of fine dust emissions by up to $\sim 0.7 \text{ kg m}^{-2}$ per month.

3.3 Spring fine dust concentrations under the high-emission scenario

Our simulations suggest that fine dust emissions will increase across arid areas in southwestern North America under RCP8.5, although only if CO₂ fertilization is of mini-

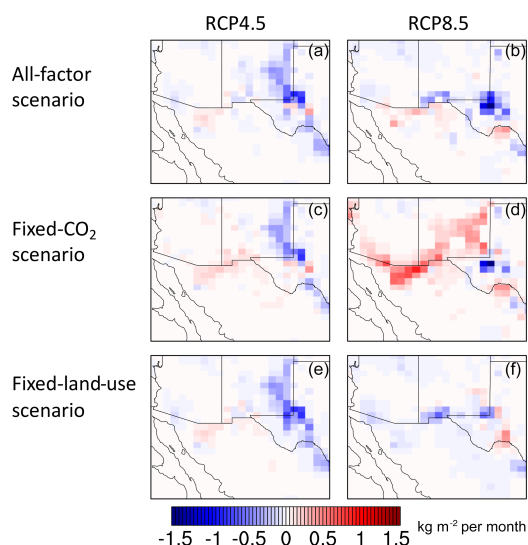


Figure 2. Simulated changes in spring averaged monthly mean dust emission in southwestern North America under the three conditions for RCP4.5 and RCP8.5. Changes are between the present day and 2100, with 5 years representing each time period. Panels (a) and (b) show results for the all-factor condition, panels (c) and (d) are for the fixed-CO₂ condition, and panels (e) and (f) are for the fixed-land-use condition. Cases are as described in Fig. 1. Results are generated offline using the GEOS-Chem emission component (HEMCO).

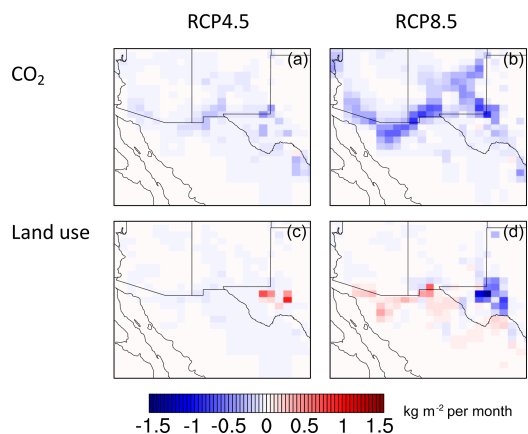


Figure 3. Contributions of CO₂ fertilization and land use change to changing dust emissions in spring in southwestern North America for RCP4.5 and RCP8.5. Changes are between the present day and 2100, with 5 years representing each time period. Panels (a) and (b) show the response of dust emission to only CO₂ fertilization, and panels (c) and (d) show the response to only trends in land use. Results are generated offline using the GEOS-Chem emission component (HEMCO).

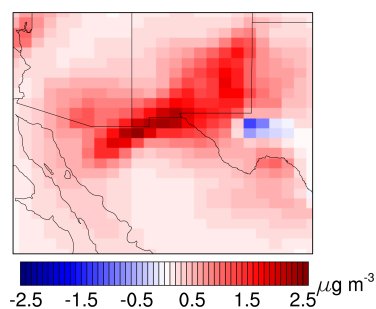


Figure 4. Simulated changes in springtime mean concentrations of fine dust over southwestern North America for the RCP8.5 fixed-CO₂ case, in which the effects of CO₂ fertilization are neglected. Changes are between the present day and 2100, with 5 years representing each time period. Results are from GEOS-Chem simulations at a $0.5^\circ \times 0.625^\circ$ resolution.

mal importance (Fig. 2). To place an upper bound on future concentrations of fine dust in this region, we apply only the fixed-CO₂ emissions to GEOS-Chem at the horizontal resolution of $0.5^\circ \times 0.625^\circ$. Given the large uncertainty in the sensitivity of vegetation to changing atmospheric CO₂ concentrations (Smith et al., 2016), we argue that this approach is justified.

Results from GEOS-Chem in the fixed-CO₂ case for RCP8.5 show that the concentrations of spring fine dust are significantly enhanced in the southeastern half of New Mexico and along the ANM border, with increases of up to $\sim 2.5 \mu\text{g m}^{-3}$ (Fig. 4). The model also yields elevated dust concentrations over nearly the entire extent of our study region by 2100. As Fig. 3 implies, anthropogenic land use along the ANM border contributes to the increased dust emissions in that area, by up to $\sim 0.7 \text{ kg m}^{-2}$ per month. Climate change impacts on natural vegetation, however, account for the bulk of the modeled increases in dust emissions in this scenario, by as much as $\sim 1.2 \text{ kg m}^{-2}$ per month (Fig. 2). The modeled wind fields, which are the same in all scenarios, transport the dust from source regions, leading to the enhanced concentrations across much of the domain, as seen in Fig. 4. We find that dust concentrations decrease only in a limited area in western Texas due to decreased pasture (Figs. 3 and S9).

4 Discussion

We apply a coupled modeling approach to investigate the impact of future changes in climate, CO₂ fertilization, and anthropogenic land use on dust mobilization and fine dust concentration in southwestern North America by the end of the 21st century. Table 1 summarizes our findings for the two RCP scenarios and three conditions – all-factor, fixed-CO₂, and fixed-land-use conditions – in spring, when dust concentrations are greatest. We find that in the RCP8.5 fixed-CO₂ scenario, in which the effects of CO₂ fertilization are ne-

glected, the VAI decreases by 26 % across the region due mainly to warmer temperatures and drier conditions, yielding an increase of 58 % in fine dust emission averaged over southwestern North America. In addition, we find that the increase in fine dust emission in northern Mexico is mainly driven by the increases in the extent of cropland and pasture cover in this area, signifying the crucial role of land use practices in modifying dust mobilization.

Our findings with respect to a diminished VAI in the future atmosphere are consistent with observed trends in vegetation during recent droughts in this region. For example, Breshears et al. (2005) documented large-scale die-off of overstorey trees across southwestern North America in 2002–2003 in response to short-term drought accompanied by bark beetle infestations. Similarly, during a multiyear (2004–2014) drought in southern Arizona, Bodner and Robles (2017) found that the spatial extent of both C₄ grass cover and shrub cover decreased in the southeastern part of that state.

The 58 % increase predicted in this study in the fixed-CO₂ RCP8.5 scenario is larger than the 26 %–46 % future increases in fine dust for this region predicted by the statistical model of Achakulwisut et al. (2018). That study relied solely on predictions of future regional-scale meteorology and did not consider the change in vegetation, as we do here. In contrast, the statistical model of Pu and Ginoux (2017) estimated a 2 % decrease in the springtime frequency of extreme dust events in the southwestern US, driven mainly by reductions in the bare-ground fraction and wind speed. Like Pu and Ginoux (2017), we also find that dust emissions decrease across a broad region of the Southwest when CO₂ fertilization is taken into account, as shown in Fig. 2. Pu and Ginoux (2017) relied on limited data for capturing the sensitivity of dust event frequency to land cover in this region, and neither that study nor Achakulwisut et al. (2018) considered changes in land use, as we do here. The direct effects of changing wind speed on dust mobilization, however, are not included in our study, but they could be tested in future work.

We further find that consideration of CO₂ fertilization can mitigate the effects of changing climate and land use on dust concentrations in southwestern North America. The all-factor and fixed-land-use simulations both yield decreases of ~20 % in mean dust emissions compared with the early 21st century. In the Intergovernmental Panel on Climate Change (IPCC) projections, CO₂ reaches ~550 ppm by 2100 under RCP4.5 and ~1960 ppm under RCP8.5 (Meinshausen et al., 2011). Correspondingly, in the RCP4.5 scenario for 2100, CO₂ fertilization enhances the VAI by 30 % in the all-factor case compared with the fixed-CO₂ case (1.07 m² m⁻² vs. 0.79 m² m⁻²); in RCP 8.5, the 2100 enhancement is 64 % (1.11 m² m⁻² vs. 0.55 m² m⁻²), as shown in Table 1. These enhancements further decrease fine dust emissions by 21 % under RCP4.5 and 78 % under RCP8.5, compared with the present day. Except along the ANM border and a few other areas, trends in land use have only minor impacts on dust mo-

bilization under the two RCPs in southwestern North America.

In summary, we find that as atmospheric CO₂ levels rise, the effect of enhanced CO₂ fertilization boosts vegetation growth and decreases dust mobilization, offsetting the impacts of warmer temperatures and reduced rainfall, at least in some areas. These results are consistent with evidence that enhanced CO₂ fertilization is already occurring in arid or semiarid environments like southwestern North America (Donohue et al., 2013; Haverd et al., 2020). In such environments, water availability is the dominant constraint on vegetation growth, and the recent enhancement of atmospheric CO₂ may have reduced stomatal conductance and limited evaporative water loss. However, the effects of CO₂ fertilization on vegetation growth are uncertain and may be attenuated by the limited supply of nitrogen and phosphorus in soil (Wieder et al., 2015). These nutritional constraints vary greatly among different PFTs (Shaw et al., 2002; Nadelhoffer et al., 1999).

Understanding the drivers in historic dust trends has sometimes been challenging (Mahowald and Luo, 2003; Mahowald et al., 2002), making it difficult to validate dust mobilization models. A further drawback of our approach is that the LPJ-LMfire model is driven by meteorological fields from just one climate model, GISS-E2-R. Given that the GISS model yields a conservative prediction of climate change in southwestern North America compared with other models (Ahlström et al., 2012; Sheffield et al., 2013), our predictions of the impact of climate change on dust mobilization may also be conservative. Other uncertainties in our study can be traced to the dust simulation. The different vegetation types in our model are quantified as fractions of grid cells, which have relatively large spatial dimensions of ~50 km × 60 km. This means the model cannot capture the spatial heterogeneity of land cover, and the aerodynamic sheltering effects of vegetation on wind erosion are neglected, as they are in most 3-D global model studies. Such sheltering could play a large role in dust mobilization (e.g., Liu et al., 1990). New methods involving satellite observations of surface albedo promise to improve understanding of the effects of aerodynamic sheltering on dust mobilization, at least for the present day (Chappell and Webb, 2016; Webb and Pierre, 2018). Implementation of aerodynamic sheltering in simulations of future climate regimes would need to account for fine-scale spatial distributions of vegetation. In addition, as recommended by Zender et al. (2003), we apply a globally uniform surface roughness Z₀ in the model, which means that the impact of changing vegetation conditions on friction velocity is not taken into account. Future work could address this weakness by varying the friction velocity according to the vegetation type. Finally, our study only focuses on the effect of changing vegetation on dust mobilization and does not consider how changing wind speeds or drier soils in the future atmosphere may more directly influence dust. Given the slight increase in monthly mean winds in RCP8.5

Table 1. The averaged spring vegetation area index (VAI) and fine dust emission in southwestern North America for the present day and future for two scenarios (RCP4.5 and RCP8.5) and three cases. The all-factor case includes changes in climate, land use, and CO₂ fertilization; the fixed-CO₂ case includes changes in only climate and land use; and the fixed-land-use case includes changes in only climate and CO₂. The rows labeled “2100–2010 (%)” give the percentage changes in the VAI and fine dust emissions between the present day and future, with positive values denoting increases in the future.

		VAI ^b (m ² m ⁻²)			Fine dust emission ^b (kg m ⁻² per month)		
		All factor	Fixed CO ₂	Fixed land use	All factor	Fixed CO ₂	Fixed land use
RCP4.5	2010 ^a	0.75 ± 0.26	0.71 ± 0.24	0.75 ± 0.26	0.10 ± 0.07	0.11 ± 0.08	0.10 ± 0.07
	2100 ^a	1.07 ± 0.48	0.79 ± 0.34	1.07 ± 0.48	0.08 ± 0.04	0.10 ± 0.05	0.08 ± 0.04
2100–2010 (%)		42	12	42	–25	–4	–26
RCP8.5	2010 ^a	0.80 ± 0.27	0.75 ± 0.24	0.75 ± 0.24	0.09 ± 0.04	0.09 ± 0.05	0.09 ± 0.04
	2100 ^a	1.11 ± 0.71	0.55 ± 0.33	0.55 ± 0.33	0.07 ± 0.04	0.14 ± 0.09	0.07 ± 0.06
2100–2010 (%)		38	–26	52	–20	58	–16

^a Each time slice represents 5 years (i.e., 2011–2015 represents the 2010 time slice, and 2095–2099 represents the 2100 time slice); ^b values are spring (MAM) averages over southwestern North America.

by 2100, future dust emissions in this scenario could be underestimated.

Within these limitations, our study quantifies the potential impacts of changing land cover and land use practices on dust mobilization and fine dust concentration over the coming century in southwestern North America. Our work builds on previous studies focused on future dust in this region by (1) more accurately capturing the transport of dust from source regions with a dynamical 3-D model, (2) considering results with and without CO₂ enhancement, and (3) including the impact of land use trends. Given the many uncertainties, it is challenging to gauge which of the three factors investigated here – climate impacts on vegetation, CO₂ fertilization, or land use change – will play the dominant role in driving future changes in dust emissions and concentrations. Thus, this study brackets a range of possible dust scenarios for southwestern North America, with the simulation without CO₂ fertilization placing an upper bound on dust emissions. In the absence of increased CO₂ fertilization, our work suggests that vegetated area will contract in response to the warmer, drier climate, exposing bare land and significantly increasing dust concentrations by 2100.

Dust enhancement could thus impose a potentially large climate penalty on PM_{2.5} air quality, with consequences for human health across much of southwestern North America, where much of the current population is of Native American and/or Latino descent. In New Mexico for example, 10 % of the population is Native American and 50 % identifies as either Hispanic or Latino. By some measures, New Mexico has also one of highest poverty rates in the US (<https://www.census.gov/quickfacts/NM>, last access: 20 August 2020). In this way, our finding of the potential for an increased dust burden in the future atmosphere has special relevance for environmental justice in this region.

Code and data availability. GEOS-Chem model codes can be obtained at <http://acmg.seas.harvard.edu/geos> (GEOS-Chem Support Team, 2020). LPJ-LMfire model codes can be obtained at <https://github.com/ARVE-Research/LPJ-LMfire> (Kaplan et al., 2018). IMPROVE datasets are available online at <http://vista.cira.colostate.edu/improve> (IMPROVE Steering Committee, 2020). The GISS-E2-R dataset was downloaded from <https://esgf-node.llnl.gov/search/cmip5/> (NASA Goddard Institute for Space Studies (GISS), 2020). The harmonized dataset of land use scenarios is available online at <http://tntcat.iiasa.ac.at/RcpDb/> (Land-use Harmonization Team, 2020). Any additional information related to this paper may be requested from the authors.

Supplement. The supplement related to this article is available online at: <https://doi.org/10.5194/acp-21-57-2021-supplement>.

Author contributions. YL conceived and designed the study, performed the GEOS-Chem simulations, analyzed the data, and wrote the paper, with contributions from all coauthors. JOK performed the LPJ-LMfire simulations. LJM conducted critical revisions of the article.

Competing interests. The authors declare that they have no conflict of interest.

Disclaimer. The views expressed in this document are solely those of the authors and do not necessarily reflect those of the EPA.

Acknowledgements. This research was developed under assistance agreements 83587501 and 83587201 awarded by the US Environmental Protection Agency (EPA). It has not been formally reviewed by the EPA. We thank all of the data providers of the datasets used in

this study. PM data were provided by the Interagency Monitoring of Protected Visual Environments (IMPROVE; available online at <http://vista.cira.colostate.edu/improve>, last access: 16 December 2020). IMPROVE is a collaborative association of state, tribal, and federal agencies, and international partners. The US Environmental Protection Agency is the primary funding source, with contracting and research support from the National Park Service. Jed O. Kaplan is grateful for access to computing resources provided by the School of Geography and the Environment, University of Oxford. The Air Quality Group at the University of California, Davis is the central analytical laboratory, with ion analysis provided by the Research Triangle Institute, and carbon analysis provided by the Desert Research Institute. We acknowledge the World Climate Research Programme's Working Group on Coupled Modelling, which is responsible for CMIP, and we thank the NASA Goddard Institute for Space Studies group for producing and making available their GISS-E2-R climate model output. For CMIP, the US Department of Energy's Program for Climate Model Diagnosis and Intercomparison provides coordinating support and led development of software infrastructure in partnership with the Global Organization for Earth System Science Portals. The GISS-E2-R dataset was downloaded from <https://esgf-node.llnl.gov/search/cmip5/> (last access: 16 December 2020). We thank the Land-use Harmonization team for producing the harmonized set of land use scenarios and making the dataset available online at <http://tntcat.iiasa.ac.at/RcpDb/> (last access: 16 December 2020). We also thank the founder, organizers, and participants of the Degree Confluence Project (<http://www.confluence.org>, last access: 16 December 2020).

Financial support. This research has been supported by the US Environmental Protection Agency (grant nos. 83587501 and 83587201).

Review statement. This paper was edited by Alex B. Guenther and reviewed by Nicholas Webb and one anonymous referee.

References

- Achakulwisut, P., Shen, L., and Mickley, L. J.: What controls springtime fine dust variability in the western United States? Investigating the 2002–2015 increase in fine dust in the U.S. Southwest, *J. Geophys. Res.-Atmos.*, 122, 12449–12467, <https://doi.org/10.1002/2017JD027208>, 2017.
- Achakulwisut, P., Mickley, L., and Anenberg, S.: Drought-sensitivity of fine dust in the US Southwest: Implications for air quality and public health under future climate change, *Environ. Res. Lett.*, 13, 054025, <https://doi.org/10.1088/1748-9326/aabf20>, 2018.
- Ahlström, A., Schurgers, G., Arneth, A., and Smith, B.: Robustness and uncertainty in terrestrial ecosystem carbon response to CMIP5 climate change projections, *Environ. Res. Lett.*, 7, 044008, <https://doi.org/10.1088/1748-9326/7/4/044008>, 2012.
- Andreadis, K. M., Clark, E. A., Wood, A. W., Hamlet, A. F., and Lettenmaier, D. P.: Twentieth-century drought in the conterminous United States, *J. Hydrometeorol.*, 6, 985–1001, 2005.
- Archer, S. R. and Predick, K. I.: Climate change and ecosystems of the southwestern United States, *Rangelands*, 30, 23–28, 2008.
- Belnap, J. and Gillette, D. A.: Vulnerability of desert biological soil crusts to wind erosion: the influences of crust development, soil texture, and disturbance, *J. Arid Environ.*, 39, 133–142, 1998.
- Bestelmeyer, B. T., Peters, D. P. C., Archer, S. R., Browning, D. M., Okin, G. S., Schooley, R. L., and Webb, N. P.: The Grassland–Shrubland Regime Shift in the Southwestern United States: Misconceptions and Their Implications for Management, *BioScience*, 68, 678–690, <https://doi.org/10.1093/biosci/biy065>, 2018.
- Bodner, G. S. and Robles, M. D.: Enduring a decade of drought: Patterns and drivers of vegetation change in a semi-arid grassland, *J. Arid Environ.*, 136, 1–14, 2017.
- Breshears, D. D., Cobb, N. S., Rich, P. M., Price, K. P., Allen, C. D., Balice, R. G., Romme, W. H., Kastens, J. H., Floyd, M. L., Belnap, J., Anderson, J. J., Myers, O. B., and Meyer, C. W.: Regional vegetation die-off in response to global-change-type drought, *P. Natl. Acad. Sci. USA*, 102, 15144–15148, <https://doi.org/10.1073/pnas.0505734102>, 2005.
- Chappell, A. and Webb, N. P.: Using albedo to reform wind erosion modelling, mapping and monitoring, *Aeolian Res.*, 23, 63–78, 2016.
- Chaste, E., Girardin, M. P., Kaplan, J. O., Bergeron, Y., and Hély, C.: Increases in heat-induced tree mortality could drive reductions of biomass resources in Canada's managed boreal forest, *Landscape Ecol.*, 34, 403–426, 2019.
- Donohue, R. J., Roderick, M. L., McVicar, T. R., and Farquhar, G. D.: Impact of CO₂ fertilization on maximum foliage cover across the globe's warm, arid environments, *Geophys. Res. Lett.*, 40, 3031–3035, 2013.
- Edwards, B., Webb, N., Brown, D., Elias, E., Peck, D., Pierson, F., Williams, C., and Herrick, J.: Climate change impacts on wind and water erosion on US rangelands, *J. Soil Water Conserv.*, 74, 405–418, 2019.
- Fairlie, T. D., Jacob, D. J., and Park, R. J.: The impact of transpacific transport of mineral dust in the United States, *Atmos. Environ.*, 41, 1251–1266, 2007.
- Gelaro, R., McCarty, W., Suarez, M. J., Todling, R., Molod, A., Takacs, L., Randles, C., Darmenov, A., Bosilovich, M. G., Reichle, R., Wargan, K., Coy, L., Cullather, R., Draper, C., Akella, S., Buchard, V., Conaty, A., da Silva, A., Gu, W., Kim, G. K., Koster, R., Lucchesi, R., Merkova, D., Nielsen, J. E., Partyka, G., Pawson, S., Putman, W., Rienecker, M., Schubert, S. D., Sienkiewicz, M., and Zhao, B.: The Modern-Era Retrospective Analysis for Research and Applications, Version 2 (MERRA-2), *J. Climate*, 30, 5419–5454, <https://doi.org/10.1175/JCLI-D-16-0758.1>, 2017.
- GEOS-Chem Support Team (Harvard University and Dalhousie University): GEOS-Chem, available at: <http://acmg.seas.harvard.edu/geos>, last access: 22 December 2020.
- Gorris, M. E., Cat, L. A., Zender, C. S., Tresseder, K. K., and Randerson, J. T.: Coccidioidomycosis Dynamics in Relation to Climate in the Southwestern United States, *Geohealth*, 2, 6–24, <https://doi.org/10.1002/2017GH000095>, 2018.
- Hand, J., White, W., Gebhart, K., Hyslop, N., Gill, T., and Schichtel, B.: Earlier onset of the spring fine dust season in the southwestern United States, *Geophys. Res. Lett.*, 43, 4001–4009, 2016.

- Hand, J., Gill, T., and Schichtel, B.: Spatial and seasonal variability in fine mineral dust and coarse aerosol mass at remote sites across the United States, *J. Geophys. Res.-Atmos.*, 122, 3080–3097, 2017.
- Harrison, S. P., Kohfeld, K. E., Roelandt, C., and Claquin, T.: The role of dust in climate changes today, at the last glacial maximum and in the future, *Earth-Sci. Rev.*, 54, 43–80, 2001.
- Haverd, V., Smith, B., Canadell, J. G., Cuntz, M., Mikaloff-Fletcher, S., Farquhar, G., Woodgate, W., Briggs, P. R., and Trudinger, C. M.: Higher than expected CO₂ fertilization inferred from leaf to global observations, *Glob. Change Biol.*, 26, 2390–2402, 2020.
- Hillel, D.: Introduction to soil physics., (Academic Press: San Diego, CA), Introduction to soil physics, Academic Press, San Diego, CA, USA, 1982.
- Hurt, G. C., Chini, L. P., Frolking, S., Betts, R., Feddema, J., Fischer, G., Fisk, J., Hibbard, K., Houghton, R., and Janetos, A.: Harmonization of land-use scenarios for the period 1500–2100: 600 years of global gridded annual land-use transitions, wood harvest, and resulting secondary lands, *Climatic Change*, 109, 117, <https://doi.org/10.1007/s10584-011-0153-2>, 2011.
- IMPROVE Steering Committee: IMPROVE datasets, available at: <http://vista.cira.colostate.edu/improve>, last access: 22 December 2020.
- Kaplan, J. O., Pfeiffer, M., and Chaste, E.: ARVE-Research/LPJ-LMfire: LPJ-LMfire (Version v1.3), Zenodo, <https://doi.org/10.5281/zenodo.1184589>, 2018.
- Klein Goldewijk, K.: Estimating global land use change over the past 300 years: the HYDE database, *Global Biogeochem. Cy.*, 15, 417–433, <https://doi.org/10.1029/1999GB001232>, 2001.
- Klein Goldewijk, K., Beusen, A., Van Dreht, G. and De Vos, M.: The HYDE 3.1 spatially explicit database of human-induced global land-use change over the past 12,000 years, *Global Ecol. Biogeogr.*, 20, 73–86, <https://doi.org/10.1111/j.1466-8238.2010.00587.x>, 2011.
- Land-use Harmonization Team: Dataset of land use scenarios, available at: <http://tntcat.iiasa.ac.at/RcpDb/>, last access: 22 December 2020.
- Li, Y., Mickley, L. J., Liu, P., and Kaplan, J. O.: Trends and spatial shifts in lightning fires and smoke concentrations in response to 21st century climate over the national forests and parks of the western United States, *Atmos. Chem. Phys.*, 20, 8827–8838, <https://doi.org/10.5194/acp-20-8827-2020>, 2020.
- Liu, S.-J., Wu, H.-I., Lytton, R. L., and Sharpe, P. J.: Aerodynamic sheltering effects of vegetative arrays on wind erosion: A numerical approach, *J. Environ. Manage.*, 30, 281–294, 1990.
- MacDonald, G. M.: Climate Change and water in Southwestern North America special feature: water, climate change, and sustainability in the southwest, *P. Natl. Acad. Sci. USA*, 107, 21256–21262, <https://doi.org/10.1073/pnas.0909651107>, 2010.
- Magi, B. I.: Global lightning parameterization from CMIP5 climate model output, *J. Atmos. Ocean. Tech.*, 32, 434–452, 2015.
- Mahowald, N. M. and Luo, C.: A less dusty future?, *Geophys. Res. Lett.*, 30, 1903, <https://doi.org/10.1029/2003GL017880>, 2003.
- Mahowald, N. M., Kohfeld, K., Hansson, M., Balkanski, Y., Harrison, S. P., Prentice, I. C., Schulz, M., and Rodhe, H.: Dust sources and deposition during the last glacial maximum and current climate: A comparison of model results with paleodata from ice cores and marine sediments, *J. Geophys. Res.-Atmos.*, 104, 15895–15916, 1999.
- Mahowald, N. M., Zender, C. S., Luo, C., Savoie, D., Torres, O., and Del Corral, J.: Understanding the 30-year Barbados desert dust record, *J. Geophys. Res.-Atmos.*, 107, AAC 7-1–AAC 7-16, 2002.
- Mahowald, N. M., Muhs, D. R., Levis, S., Rasch, P. J., Yoshioka, M., Zender, C. S., and Luo, C.: Change in atmospheric mineral aerosols in response to climate: Last glacial period, preindustrial, modern, and doubled carbon dioxide climates, *J. Geophys. Res.-Atmos.*, 111, D10202, <https://doi.org/10.1029/2005JD006653>, 2006.
- McClaran, M. P. and Van Devender, T. R.: The desert grassland, University of Arizona Press, Tucson, AZ, USA, 1997.
- Meinshausen, M., Smith, S. J., Calvin, K., Daniel, J. S., Kainuma, M., Lamarque, J.-F., Matsumoto, K., Montzka, S., Raper, S., and Riahi, K.: The RCP greenhouse gas concentrations and their extensions from 1765 to 2300, *Climatic Change*, 109, 213, <https://doi.org/10.1007/s10584-011-0156-z>, 2011.
- Meng, Z. and Lu, B.: Dust events as a risk factor for daily hospitalization for respiratory and cardiovascular diseases in Minqin, China, *Atmos. Environ.*, 41, 7048–7058, 2007.
- Nadelhoffer, K. J., Emmett, B. A., Gundersen, P., Kjonaas, O. J., Koopmans, C. J., Schleiippi, P., Tietema, A., and Wright, R. F.: Nitrogen deposition makes a minor contribution to carbon sequestration in temperate forests, *Nature*, 398, 145–148, <https://doi.org/10.1038/18205>, 1999.
- NASA Goddard Institute for Space Studies (GISS): GISS-E2-R dataset, available at: <https://esgf-node.lnl.gov/search/cmip5/>, last access: 22 December 2020.
- Nazarenko, L., Schmidt, G., Miller, R., Tausnev, N., Kelley, M., Ruedy, R., Russell, G., Aleinov, I., Bauer, M., and Bauer, S.: Future climate change under RCP emission scenarios with GISS ModelE2, *J. Adv. Model. Earth Syst.*, 7, 244–267, 2015.
- Nicholson, S. E., Tucker, C. J., and Ba, M.: Desertification, drought, and surface vegetation: An example from the West African Sahel, *B. Am. Meteorol. Soc.*, 79, 815–830, 1998.
- Park, R. J., Jacob, D. J., Field, B. D., Yantosca, R. M., and Chin, M.: Natural and transboundary pollution influences on sulfate-nitrate-ammonium aerosols in the United States: Implications for policy, *J. Geophys. Res.-Atmos.*, 109, D15204, <https://doi.org/10.1029/2003JD004473>, 2004.
- Pfeiffer, M., Spessa, A., and Kaplan, J. O.: A model for global biomass burning in preindustrial time: LPJ-LMfire (v1.0), *Geosci. Model Dev.*, 6, 643–685, <https://doi.org/10.5194/gmd-6-643-2013>, 2013.
- Polley, H. W., Briske, D. D., Morgan, J. A., Wolter, K., Bailey, D. W., and Brown, J. R.: Climate change and North American rangelands: trends, projections, and implications, *Rangeland Ecol. Manag.*, 66, 493–511, 2013.
- Poorter, H. and Perez-Soba, M.: Plant growth at elevated CO₂, *Encyclopedia of global environmental change*, 2, 489–496, 2002.
- Prein, A. F., Holland, G. J., Rasmussen, R. M., Clark, M. P., and Tye, M. R.: Running dry: The US Southwest's drift into a drier climate state, *Geophys. Res. Lett.*, 43, 1272–1279, 2016.
- Pu, B. and Ginoux, P.: Projection of American dustiness in the late 21(st) century due to climate change, *Sci. Rep.*, 7, 5553, <https://doi.org/10.1038/s41598-017-05431-9>, 2017.
- Raupach, M.: Simplified expressions for vegetation roughness length and zero-plane displacement as functions of canopy height and area index, *Bound.-Lay. Meteorol.*, 71, 211–216, 1994.

- Ridley, D. A., Heald, C. L., Pierce, J., and Evans, M.: Toward resolution-independent dust emissions in global models: Impacts on the seasonal and spatial distribution of dust, *Geophys. Res. Lett.*, 40, 2873–2877, 2013.
- Seager, R. and Vecchi, G. A.: Greenhouse warming and the 21st century hydroclimate of southwestern North America, *P. Natl. Acad. Sci. USA*, 107, 21277–21282, <https://doi.org/10.1073/pnas.0910856107>, 2010.
- Shaw, M. R., Zavaleta, E. S., Chiariello, N. R., Cleland, E. E., Mooney, H. A., and Field, C. B.: Grassland responses to global environmental changes suppressed by elevated CO₂, *Science*, 298, 1987–1990, <https://doi.org/10.1126/science.1075312>, 2002.
- Sheffield, J., Barrett, A. P., Colle, B., Nelun Fernando, D., Fu, R., Geil, K. L., Hu, Q., Kinter, J., Kumar, S., and Langenbrunner, B.: North American climate in CMIP5 experiments. Part I: Evaluation of historical simulations of continental and regional climatology, *J. Climate*, 26, 9209–9245, 2013.
- Sitch, S., Smith, B., Prentice, I. C., Arneth, A., Bondeau, A., Cramer, W., Kaplan, J. O., Levis, S., Lucht, W., Sykes, M. T., Thonicke, K., and Venevsky, S.: Evaluation of ecosystem dynamics, plant geography and terrestrial carbon cycling in the LPJ dynamic global vegetation model, *Glob. Change Biol.*, 9, 161–185, <https://doi.org/10.1046/j.1365-2486.2003.00569.x>, 2003.
- Smith, W. K., Reed, S. C., Cleveland, C. C., Ballantyne, A. P., Anderegg, W. R., Wieder, W. R., Liu, Y. Y., and Running, S. W.: Large divergence of satellite and Earth system model estimates of global terrestrial CO₂ fertilization, *Nat. Clim. Change*, 6, 306–310, 2016.
- Stahle, D. W.: Anthropogenic megadrought, *Science*, 368, 238–239, <https://doi.org/10.1126/science.abb6902>, 2020.
- Tegen, I., Werner, M., Harrison, S., and Kohfeld, K.: Relative importance of climate and land use in determining present and future global soil dust emission, *Geophys. Res. Lett.*, 31, L05105, <https://doi.org/10.1029/2003GL019216>, 2004.
- Tong, D. Q., Wang, J. X. L., Gill, T. E., Lei, H., and Wang, B.: Intensified dust storm activity and Valley fever infection in the southwestern United States, *Geophys. Res. Lett.*, 44, 4304–4312, <https://doi.org/10.1002/2017GL073524>, 2017.
- Van Loon, A. F., Stahl, K., Di Baldassarre, G., Clark, J., Rango-croft, S., Wanders, N., Gleeson, T., Van Dijk, A. I. J. M., Tallaksen, L. M., Hannaford, J., Uijlenhoet, R., Teuling, A. J., Hannah, D. M., Sheffield, J., Svoboda, M., Verbeiren, B., Wagener, T., and Van Lanen, H. A. J.: Drought in a human-modified world: reframing drought definitions, understanding, and analysis approaches, *Hydrol. Earth Syst. Sci.*, 20, 3631–3650, <https://doi.org/10.5194/hess-20-3631-2016>, 2016.
- Webb, N. P. and Pierre, C.: Quantifying anthropogenic dust emissions, *Earth's Future*, 6, 286–295, 2018.
- Wieder, W. R., Cleveland, C. C., Smith, W. K., and Todd-Brown, K.: Future productivity and carbon storage limited by terrestrial nutrient availability, *Nat. Geosci.*, 8, 441–444, 2015.
- Williams, A. P., Allen, C. D., Macalady, A. K., Griffin, D., Woodhouse, C. A., Meko, D. M., Swetnam, T. W., Rauscher, S. A., Seager, R., and Grissino-Mayer, H. D.: Temperature as a potent driver of regional forest drought stress and tree mortality, *Nat. Clim. Change*, 3, 292–297, 2013.
- Williams, A. P., Cook, E. R., Smerdon, J. E., Cook, B. I., Abatzoglou, J. T., Bolles, K., Baek, S. H., Badger, A. M., and Livneh, B.: Large contribution from anthropogenic warming to an emerging North American megadrought, *Science*, 368, 314–318, 2020.
- Woodward, S., Roberts, D., and Betts, R.: A simulation of the effect of climate change-induced desertification on mineral dust aerosol, *Geophys. Res. Lett.*, 32, L18810, <https://doi.org/10.1029/2005GL023482>, 2005.
- Zender, C. S., Bian, H., and Newman, D.: Mineral Dust Entrainment and Deposition (DEAD) model: Description and 1990s dust climatology, *J. Geophys. Res.-Atmos.*, 108, 4416, <https://doi.org/10.1029/2002JD002775>, 2003.
- Zeng, X., Shaikh, M., Dai, Y., Dickinson, R. E., and Myneni, R.: Coupling of the common land model to the NCAR community climate model, *J. Climate*, 15, 1832–1854, 2002.